Pharmaceutical Research, Vol. 22, No. 10, October 2005 (© 2005)
DOI: 10.1007/s11095-005-6807-x

Research Paper

Pharmacokinetic Differences between Pantoprazole Enantiomers in Rats

Zhiyong Xie,[1] Yini Zhang,[1] Haiyan Xu,[1] and Dafang Zhong[1,2]

Received March 29, 2005; accepted June 21, 2005

Purpose. The purpose of this study was to quantitatively clarify the contribution of the absorption, protein binding, and metabolism of cytochrome P450 enzymes to the enantioselective pharmacokinetics of pantoprazole enantiomers in rats.
Methods. The enantioselective pharmacokinetics of pantoprazole enantiomers was estimated by an oral administration of racemic pantoprazole to rats. The pharmacokinetic differences between pantoprazole enantiomers were evaluated by the experiments of the *in situ* perfusion into rat small intestine, the protein binding, and the *in vitro* metabolism in rat liver microsomes of pantoprazole enantiomers.
Results. The mean area under the curve value of *S*-pantoprazole was 1.5 times greater than that of *R*-pantoprazole after administration of racemic pantoprazole to rats (20 mg/kg, p.o.). There were significant differences in k_e ($p < 0.05$), $t_{1/2}$ ($p < 0.01$), and mean residence time ($p < 0.01$) values between the two enantiomers. In the *in situ* absorption study, the absorption rate constants were of no significant differences between the two enantiomers. The mean unbound fraction of *R*-pantoprazole was slightly greater than that of *S*-pantoprazole. The intrinsic clearance (CL_{int}) of the formation of the 5′-*O*-demethyl metabolite from *S*-pantoprazole was 4-fold lower than that from *R*-pantoprazole. However, the CL_{int} value for the sulfone and 6-hydroxy metabolites from *S*-pantoprazole was higher than that from *R*-pantoprazole. The sum of the CL_{int} of the formation of all three metabolites was 3.06 and 4.82 mL/min/mg protein for *S*- and *R*-pantoprazole, respectively.
Conclusions. This study suggests that the enantioselective pharmacokinetics of pantoprazole enantiomers in rats is probably ascribable to their enantioselective metabolism, which is contributed by all the three metabolic pathways, including sulfoxide oxidation, 4′-*O*-demethylation, and 6-hydroxylation.

KEY WORDS: enantiomer; enantioselectivity; metabolism; pantoprazole; pharmacokinetics.

INTRODUCTION

Pantoprazole, a benzimidazole derivative that powerfully and continuously inhibits gastric proton-pump (H^+/K^+-ATPase) activity in the final step of gastric acid secretion in the parietal cells (1), is used clinically in the treatment of reflux esophagitis, Zollinger–Ellison syndrome, peptic ulcers, and other acid-related, hypersecretory gastrointestinal disorders (2,3). The drug is extensively metabolized in liver. The major metabolic pathways include sulfoxide oxidation and reduction (catalyzed mainly by CYP3A4), 4′-*O*-demethylation, and aromatic hydroxylation (catalyzed by CYP2C19) (4). All proton pump inhibitors (PPIs), including omeprazole, pantoprazole, lansoprazole, and rabeprazole, have a common chiral benzimidazole sulfoxide structure. They have, however, been used as racemic mixtures of the stereoisomers. There are a few reports on the *in vivo* pharmacokinetics of the individual optical isomers obtained by enantioselective analysis of plasma after administration of the racemates of omeprazole (5,6), pantoprazole (7,8), and lansoprazole (9,10) in humans and rabeprazole in rats (11) and in dogs (11,12). These results obtained from above studies in humans indicated that in extensive metabolizers (EMs), the area under the plasma concentration *vs.* time curves (AUCs) were higher for the *S*-enantiomers of omeprazole and pantoprazole than for the respective *R*-enantiomer, whereas in poor metabolizers (PMs), the AUCs were significantly higher for the *R*-enantiomers than for the respective *S*-enantiomer. However, the plasma concentrations of the *R*-enantiomer of lansoprazole were consistently higher than those of the *S*-enantiomer in both CYP2C19 EMs and PMs, which suggested that CYP2C19-mediated enantioselective metabolism of lansoprazole was different from that of omeprazole and pantoprazole. This was because of the well-known reason that enantiomer-selective disposition of PPIs was highly dependent on CYP2C19 genetic polymorphism. Some other studies on the enantioselective metabolism of omeprazole (13), lansoprazole (14–16), and a structurally analogous compound of PPIs (H 285/31, 5-fluoro-2-[[(4-cyclopropylmethoxy-2-pyridinyl)methyl]sulfinyl]-1*H*-benzimidazole) (17) in liver microsomes of different species indicated a significant enantioselectivity in the metabolism of enantiomers of these drugs. In the studies by the cDNA-expressed enzymes (13–17), the enzymes that mediated the

[1] Laboratory of Drug Metabolism and Pharmacokinetics, Shenyang Pharmaceutical University, 103 Wenhua Road, Shenyang, 110016 People's Republic of China.
[2] To whom correspondence should be addressed. (e-mail: zhongdf@china.com).

sulfone formation and hydroxylation of PPIs were identified to be CYP3A4 and CYP2C19, respectively. The intrinsic clearance (CL_{int}) for the *S*-omeprazole was approximately three times lower than that of the *R*-omeprazole, which was mainly due to the considerably lower formation ratio of 5-hydroxylate metabolite from *S*-omeprazole than that from *R*-omeprazole (the formation ratios of other metabolites were comparative) (13). However, the studies on pharmacokinetic difference of lansoprazole in rats (14), in dogs (15), and in humans (16) clearly demonstrated stereoselectivity in the protein binding and the formation of both hydroxylate metabolite and sulfone from lansoprazole enantiomers. The two formation ratios of the above metabolites were consistently and significantly higher for the *S*-lansoprazole than those for the *R*-enantiomer in human liver microsomes (16). Taken together, the observations on the stereoselectivity in the human CYP2C19-mediated metabolism of PPIs indicated that *R*-enantiomers were preferentially metabolized in the pyridine group, whereas *S*-enantiomers were subject to metabolism in the benzimidazole by CYP2C19 enzyme (17). Because limited information is available about the potential differences in pharmacokinetics and pharmacodynamics between pantoprazole enantiomers, it is important to evaluate the pharmacokinetics of the individual enantiomers because the pharmacological effects or toxicity, or both, of the enantiomers might be different. To date, there are two papers on the enantioselective pharmacokinetics of pantoprazole in EMs and PMs published (7,8). In the EMs, the AUC of *S*-pantoprazole was slightly higher than that of *R*-pantoprazole, indicating that the *S*-enantiomer is a more favorable one of the two enantiomers. However, significant differences in the AUCs (approximately three times greater for the *R*-pantoprazole than that for the *S*-pantoprazole) were observed in the PMs, in which enantioselective metabolism was mainly mediated via CYP3A4 but not CYP2C19. Masubuchi *et al.* (18) have reported that significant chiral inversion occurred after intravenous and oral administration of *R*-pantoprazole to male Sprague–Dawley rats.

In the present study, we extend the previous work on the enantioselective differences between pantoprazole enantiomers in the pharmacokinetic behaviors, i.e., absorption, protein binding, and metabolism of cytochrome P450 (CYP450) enzymes to the enantioselective metabolism in Wistar rats.

MATERIALS AND METHODS

Materials

Racemic pantoprazole sodium (purity 99.5%) and racemic omeprazole magnesium (purity 99.2%) were purchased from Dongyu Pharmaceutical Co. Ltd. (Shenyang, China). (+)-Pantoprazole sodium (enantiomeric purity 98.5%), (−)-pantoprazole sodium (enantiomeric purity 98.1%) [the absolute configuration of the optical isomers of pantoprazole has not been published, but, by analogy to other PPIs and as discussed previously (13,17), it is highly probable that (+)-pantoprazole is of the *R*-configuration], pantoprazole sulfone, and pantoprazole sulfide were synthesized at the School of Pharmaceutical Engineering, Shenyang Pharmaceutical University (Shenyang, China). Reference substances of two pantoprazole metabolites, 4′-*O*-demethyl-pantoprazole sulfide and 6-hydroxy-pantoprazole, were isolated from urine of rats after oral administration of racemic pantoprazole sodium, and their structures were identified by nuclear magnetic resonance (NMR). Nicotinamide adenine dinucleotide phosphate (NADPH) was obtained from Xinjingke Biotechnology Co. Ltd. (Beijing, China). Methanol and acetonitrile, purchased from Concord Technology Co. Ltd. (Tianjin, China), were of high-performance liquid chromatography (HPLC) grade. Other reagents were of analytical grade and could be obtained commercially.

Animals

Male Wistar rats, purchased from the Experimental Animal Center of Shenyang Pharmaceutical University (Shenyang, China), were housed in a light- and humidity-controlled animal facility. All the procedures involving animals adhered to the Principles of Laboratory Animal Care (NIH publication #85-23, revised in 1985) and approved by the Animal Ethics Committee of Shenyang Pharmaceutical University.

In Vivo Experiments

Eight male Wistar rats (200–250 g), which were maintained on standard food, were fasted 12 h with free access to water before performance of the experiment. Each rat was orally administered with 20 mg/kg racemic pantoprazole (pantoprazole sodium was dissolved in saline containing 0.5% 1 M NaOH and 5% ethanol). Blood samples (250 μL) were collected from jugular vein before (0 h) and at 1, 5, 15, 30, and 45 min, 1.0, 1.5, 2.0, 3.0, 5.0, and 8.0 h after dosing. All blood samples were heparinized and were immediately centrifuged for 5 min (2,500 × *g*). The supernatant plasma was isolated in other tubes and then frozen at −20°C before measurement.

In Situ Perfusion into Rat Small Intestinal Tract

Male Wistar rats (200–250 g), which were maintained on standard food, were fasted 12 h before the experiment. The perfused small intestine was prepared according to the method reported (19). Briefly, after anesthetizing the rat with ethyl carbamate (urethane, 1.2 g/kg, i.p.), the small intestine was exposed by midline abdominal incision, and the upper duodenum and the ileocaecal junction were cannulated with polyethylene tubing. Lactated Ringer's solution (pH 7.4, maintained at 37°C; 100 mL) containing racemic pantoprazole (50 μg/mL) was perfused from the duodenum through the small intestine to the ileocaecal junction at a rate of 5 mL/min. The concentrations of pantoprazole enantiomers in the perfusates were determined, and the volumes of perfusates were recorded at each time, respectively. The absorption rate constant (k_a) was obtained by use of the equation: $k_a = \ln(C_0V_0/C_1V_1)/t$, where t is the perfusion time, C_0 and C_1 are the concentrations of pantoprazole enantiomers in the perfusates at 0 and 90 min, respectively, and V_0 and V_1 are the volumes of the perfusates at 0 and 90 min, respectively.

Protein Binding Experiments

The protein binding experiments were performed using racemic pantoprazole at 1.0, 2.0, 4.0, and 8.0 μg/mL of pantoprazole enantiomers in freshly obtained rat plasma with an equilibrium dialysis method in five replicates, and the equilibrium dialysis was carried out in a Diachem M_w: 10,000 high permeability membranes.

Dialysis of buffer solution (pH 7.4) against plasma-contained pantoprazole enantiomers was performed for 48 h at 4°C. Significant volume shifts or adsorption losses were not observed after dialysis. The fraction of the unbound drug was determined by use of the equation: $f_u = C_u/C_t$, where f_u is the fraction of unbound drug in plasma and C_u and C_t refer to the unbound and total concentration of the drug in plasma after equilibrium dialysis, respectively.

Preparation of Rat Liver Microsomes

The rat liver microsomes were prepared from male Wistar rats according to the method of Ernster *et al.* (20), and the microsomal protein concentration was measured according to Lowry *et al.* (21) using bovine serum albumin as standard. After determination of protein concentration, the microsomal suspension was kept at −80°C until used.

Incubation of Pantoprazole Enantiomers with Rat Liver Microsomes

The basic incubation medium contained 0.1 M Tris–HCl buffer (pH 7.4), 1.0 mM NADPH, 10 mM KCl and 10 mM $MgCl_2$, 1.0 mg/mL microsomal protein, and pantoprazole enantiomers (10–600 μM) in a final volume of 200 μL. The mixture was incubated at 37°C for 40 min. The reactions were initiated by addition of 1.0 mM NADPH after a 5-min preincubation and were terminated with 3 mL of an *n*-hexane–dichloromethane–2-propanol (20:10:1, v/v/v) mixture. Internal standard (omeprazole, 100 μL, 8.0 μg/mL) was added to the mixtures. After liquid–liquid extraction, the supernatant was evaporated to dryness under a stream of nitrogen at 40°C. The residue was dissolved in 100 μL of acetonitrile–water (90:10, v/v) for LC-MS-MS assay. Controls were conducted in the same manner, except for the presence of the NADPH. Blank samples were assayed without substrate to be able to exclude analytical interferences by the matrix. All experiments were performed in triplicate.

Enzyme Kinetics Studies

For the kinetic experiments, linearity in the formation rate of metabolites was established with respect to microsomal protein concentration and incubation time. The rate of formation was linear over 60-min incubation and 0.5–1.5 mg/mL of microsomal protein. Twelve different concentrations, ranging from 10 to 600 μM, were used in the V_m/K_m determination. Enzyme kinetic parameters were obtained by a nonlinear least-squares program MULTI (22). The Michaelis–Menten equation, $V = V_mS/(K_m + S)$, was fitted to the formation rate of the reaction at substrate concentration S; V_m is the maximum velocity, and K_m is the substrate concentration at which the reaction velocity is 50% of V_m. Intrinsic clearance of the *in vitro* incubation was calculated as $CL_{int} = V_m/K_m$.

Determination of Pantoprazole in Plasma, Perfusate, and Dialysis Solutions

Determination of pantoprazole enantiomers in plasma (100 μL), perfusate solution (100 μL), and dialysis solution (1 mL) was performed using reversed-phase high-performance liquid chromatography (an HP 1100 system equipped with a G1314A UV-detector, a G1313A quaternary pump, a G1313A autosampler, a G1316A column oven, and a vacuum degasser unit). To a 10-mL centrifuge tube containing 0.8 μg internal standard (omeprazole) and 200 μL potassium dihydrogen phosphate buffer (pH 7.0), one of the three samples (plasma, perfusate solution, or dialysis solution) and 3 mL of an *n*-hexane–dichloromethane–2-propanol (20:10:1, v/v/v) mixture were added. The resulting mixture was shaken for 30 s and centrifuged (2,500 × *g*) for 10 min. The organic layer was transferred to another test tube and evaporated. The residue was reconstituted in 100 μL of a 10 mM ammonium acetate buffer (pH 6.5)–acetonitrile (35:65, v/v) mixture. A 50-μL aliquot was injected onto the HPLC column. The chromatographic separation was performed on a Diamonsil C_{18} column (250 × 4.0 mm I.D., 5 μm, Dikma, Beijing, China). The mobile phase consisted of 10 mM ammonium acetate buffer (pH 6.5) and acetonitrile (35:65, v/v). At a flow rate of 1.0 mL/min, the eluate was monitored for absorbance at 290 nm, and the portion eluted over 1 min of the peak of racemic pantoprazole was collected. The collected eluate was subjected to the same process as the preparation of plasma samples. The residue was then reconstituted in a 100-μL mixture of a 10 mM ammonium acetate buffer (pH 6.5) and acetonitrile (93:7, v/v), and a 50-μL aliquot was injected onto the chiral HPLC system. Determination of pantoprazole enantiomers was performed on a Chiral-AGP column (150 × 4.0 mm I.D., 5 μm, ChromTech, Haegersten, Sweden) with a Chiral-AGP guard column (10 × 3 mm I.D., ChromTech). The mobile phase was 10 mM ammonium acetate buffer (pH 6.5)–acetonitrile (93:7, v/v), and its flow rate was 0.9 mL/min. The Chiral-AGP column was maintained at 20°C.

Determination of Pantoprazole Metabolites in Microsomal Mixtures

The concentrations of pantoprazole metabolites formed from rat liver microsomes were determined according to standard curves by an LC/MS/MS method using selected reaction monitoring mode, which was performed on a Thermo-Finnigan LCQ ion trap mass spectrometer (San Jose, CA, USA) equipped with an electrospray ionization (ESI) source. The column was a Diamonsil C_{18} column (250 × 4.0 mm I.D., 5 μm, Dikma) preceded by a Hypersil BDS-C_{18} precolumn (10 × 4.6 mm I.D., 5 μm). The mobile phase consisting of acetonitrile–water (90:10, v/v) was delivered by a Shimadzu LC-10AD (Kyoto, Japan) pump at a flow rate of 0.5 mL/min. The parameters of the selected reaction monitoring transitions for the $[M + H]^+$ to selected product ions were optimized with the following typical values for the analytes and internal standard (each at its optimum collision

energy): pantoprazole sulfone *m/z* 400–336; 4′-*O*-demethyl-pantoprazole sulfide *m/z* 354–321; 6-hydroxy-pantoprazole *m/z* 400–200; and the internal standard omeprazole *m/z* 346–198. Instrument control, data acquisition, and data evaluation were performed using Navigator software (version 1.2, Finnigan). In this study, the lower limit of quantification was 100 nM for all the three metabolites of pantoprazole.

Pharmacokinetic Analysis

All data were analyzed by noncompartmental analysis using the TopFit 2.0 software package (Thomae GmbH, Germany). The maximum plasma concentration (C_{max}) and the time to reach C_{max} (t_{max}) were obtained graphically. The elimination rate constant (k_e) was determined by the least-squares regression of the logarithm of plasma concentration time over four terminal points. The area under the plasma concentration time curves ($AUC_{0-\infty}$) were calculated using the trapezoidal rule and by extrapolating the time to infinity using the elimination rate constant (k_e) values. The terminal half-life ($t_{1/2}$) was calculated by dividing 0.693 by k_e. The apparent total body clearance (CL_{tot}/F) was calculated from CL_{tot}/F = Dose/$AUC_{0-\infty}$, where F (bioavailability) is the fraction of the dose absorbed. In this study, we did not take the body weight into consideration when analyzing pharmacokinetic parameters because there was little correlation between AUC and body weight.

Statistical Analysis

Each result is expressed as a mean ± SD. Pharmacokinetic data were analyzed for statistical differences using Student's t test. Statistical significance was assumed when $p < 0.05$.

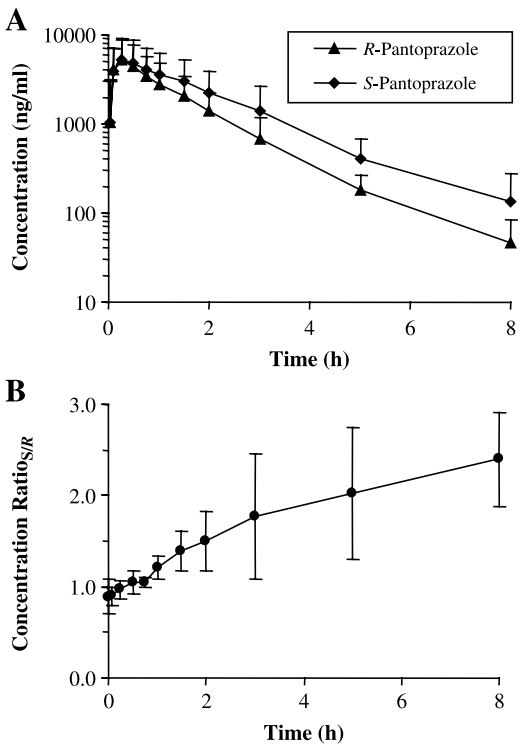

Fig. 1. Plasma concentration-time (A) and ratio$_{S/R}$-time (B) profiles of the enantiomers of pantoprazole after an oral administration of 20 mg/kg of racemic pantoprazole to Wistar rats (n = 8).

Table I. Pharmacokinetic Parameters of *S*- and *R*-Pantoprazole After an Oral Administration of 20 mg/kg of Racemic Pantoprazole to Wistar Rats (Mean ± SD, n = 8)

Parameter	*S*-Pantoprazole	*R*-Pantoprazole	Ratio$_{S/R}$
$t_{1/2}$ (h^{-1})	1.46 ± 0.32	1.33 ± 0.36[a]	1.10 ± 0.06
k_e (h^{-1})	0.49 ± 0.10	0.55 ± 0.14[b]	0.89 ± 0.07
t_{max} (h)	0.21 ± 0.15	0.18 ± 0.09[c]	1.17 ± 0.19
C_{max} (μg/mL)	5.00 ± 3.80	4.91 ± 3.41[c]	1.01 ± 0.10
AUC_{0-t} (μg h/mL)	10.86 ± 8.87	7.46 ± 5.29[b]	1.46 ± 0.16
$AUC_{0-\infty}$(μg h/mL)	11.01 ± 8.90	7.52 ± 5.29[b]	1.46 ± 0.16
MRT (h)	2.08 ± 0.37	1.67 ± 0.33[a]	1.25 ± 0.04
CL/F (mL/min/kg)	27.28 ± 20.31	34.87 ± 22.40[c]	0.78 ± 0.29
V_d/F (L/kg)	3.89 ± 3.51	4.58 ± 3.74[c]	0.85 ± 0.30
F	86.5	85.4	1.01

[a] $p < 0.01$ *vs. S*-pantoprazole.
[b] $p < 0.05$ *vs. S*-pantoprazole.
[c] $p > 0.05$ *vs. S*-pantoprazole.

RESULTS

In Vivo Experiments

Pharmacokinetic behaviors of both enantiomers of pantoprazole in Wistar rats, following an oral administration of 20 mg/kg of racemic pantoprazole, are shown in Fig. 1. The mean plasma concentrations of *S*-pantoprazole tended to be higher than those of *R*-pantoprazole, and the mean plasma concentration ratio of *S*-pantoprazole to *R*-enantiomer (ratio$_{S/R}$) was not constant and changed with time. The initial plasma concentration ratio$_{S/R}$ was close to 1.0 and gradually increased to 2.4 (8.0 h after the dosing) with time. The pharmacokinetic parameters and the concentration ratio$_{S/R}$ are summarized in Table I. Plasma concentration of *R*-pantoprazole reached a C_{max} of 4.91 ± 3.41 μg/mL at 0.18 ± 0.09 h (t_{max}) after dosing and decreased with a terminal $t_{1/2}$ of about 1.33 ± 0.36 h. That of *S*-pantoprazole reached a C_{max} of 5.00 ± 3.80 μg/mL at 0.21 ± 0.15 h (t_{max}) after dosing and decreased with a terminal $t_{1/2}$ of about 1.46 ± 0.32 h. There were no significant differences in C_{max}, t_{max}, CL_{tot}/F, V_d/F, and F values between the two enantiomers of pantoprazole, whereas there were significant differences in AUC_{0-t}, $AUC_{0-\infty}$, k_e, $t_{1/2}$, and mean residence time (MRT) values between them. The mean ratios$_{S/R}$ for the AUC_{0-t}, $AUC_{0-\infty}$, k_e, $t_{1/2}$, and MRT were 1.46 ± 0.16, 1.46 ± 0.16, 0.89 ± 0.07, 1.10 ± 0.06, and 1.25 ± 0.04, respectively.

In Situ Perfusion into Rat Small Intestinal Tract

The enantioselectivity in the intestinal absorption of pantoprazole was investigated by the *in situ* recirculation method. There was no significant difference in the absorption between the two enantiomers of pantoprazole. The average absorption rate constants (k_a) of *R*- and *S*-pantoprazole were 0.44 ± 0.04 and 0.41 ± 0.06 h^{-1}, respectively (n = 4, $p > 0.05$).

Protein Binding Experiments

To ensure the investigated concentrations consistent with the enantiomers plasma concentration range (50–10,000 ng/

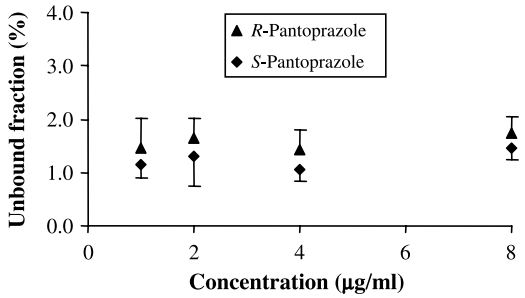

Fig. 2. Enantioselective binding of *R*-pantoprazole and *S*-pantoprazole to rat plasma proteins (initial plasma concentrations of pantoprazole enantiomers were 1.0, 2.0, 4.0, and 8.0 μg/mL, mean ± SD, $n = 5$).

mL) after an oral dose of 20 mg/kg racemic pantoprazole to Wistar rats, and because an interaction between the enantiomers might occur, the protein binding experiments were performed using racemic pantoprazole at 1.0, 2.0, 4.0, and 8.0 μg/mL of pantoprazole enantiomers in freshly obtained rat plasma. The extent of enantioselective binding of *S*-pantoprazole to rat plasma protein was slightly greater than that of *R*-enantiomer. Unbound fractions of *S*-pantoprazole were 1.15, 1.29, 1.05, and 1.46% at initial plasma concentrations 1.0, 2.0, 4.0, and 8.0 μg/mL of pantoprazole enantiomers, respectively, whereas those of *R*-pantoprazole were 1.46, 1.63, 1.41, and 1.74% (Fig. 2). There was no significant difference in the unbound fraction between the two enantiomers of pantoprazole ($n = 5$, $p > 0.05$).

In Vitro Metabolic Experiments Using Rat Liver Microsomes

In this study, sulfoxidation to sulfone, 4′-*O*-demethylation to 4′-*O*-demethyl-pantoprazole sulfide, and aromatic hydroxylation to 6-hydroxy-pantoprazole were identified as the main metabolic pathways of pantoprazole. A fourth minor metabolite was identified as pantoprazole sulfide, and other minor metabolites were detected but not identified (Fig. 3). The above four metabolites were identified by LC/MS^n and comparison of LC retention times with reference substances. The formation of the three main metabolites (sulfone, 6-hydroxy, and 4′-*O*-demethyl metabolites) from *S*- and *R*-pantoprazole was further studied using rat liver microsomes, respectively. The V_m, K_m, and CL_{int} values of the formation of all three metabolites from *S*-pantoprazole and *R*-enantiomer in rat liver microsomes are presented in Table II. The CL_{int} values showed that the three metabolites formed from *S*-pantoprazole were equally important for its elimination, whereas the 4′-*O*-demethyl metabolite dominated the elimination of *R*-pantoprazole. The sum of the formation CL_{int} of all three metabolites was 3.06 and 4.80 μL/min/mg of protein for *S*- and *R*-pantoprazole, respectively, indicating enantioselectivity in the metabolism, and the *S*-pantoprazole was cleared more slowly than *R*-pantoprazole. Representative saturation curves for the formation of the metabolites from the pooled rat liver microsomes are shown in Fig. 4. The K_m values evaluated for the formation of the 4′-*O*-demethyl metabolite seem to be lower for *R*-pantoprazole than for *S*-pantoprazole, whereas the K_m values evaluated for the formation of the sulfone seem to be higher for *R*-pantoprazole than for *S*-pantoprazole.

DISCUSSION

In this study, the stereoselectivity of pantoprazole pharmacokinetics in Wistar rats after oral administration of racemic pantoprazole was investigated. The AUC value of *S*-pantoprazole was 1.5-fold greater than that of *R*-pantopra-

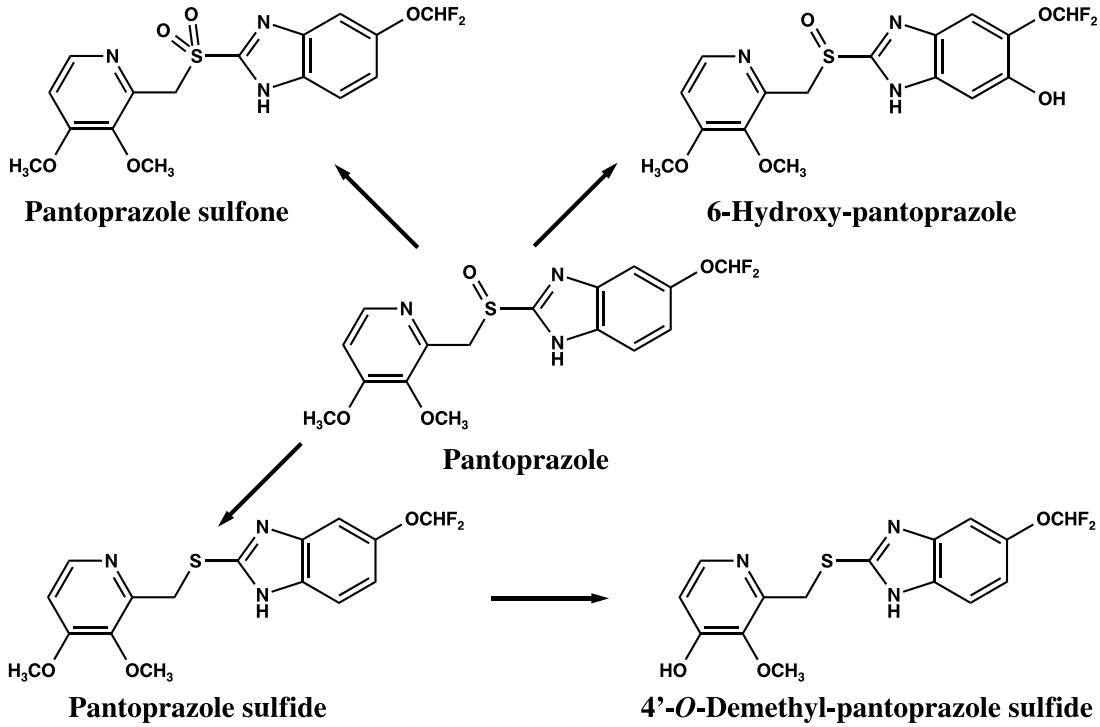

Fig. 3. Structures of pantoprazole and its metabolites produced by incubation in rat liver microsomes.

Table II. Enzyme Kinetic Parameters of the Formation of Metabolites from *S*-Pantoprazole and *R*-Pantoprazole in Rat Liver Microsomes (K_m expressed as μmol/L, V_m as nmol/mg of protein, and CL_{int} as μL/min/mg of microsomal protein)

Metabolite	Parameter	*S*-Pantoprazole	% of Sum	*R*-Pantoprazole	% of Sum
Sulfone	V_m	236.3		205.0	
	K_m	167.5		303.5	
	CL_{int}	1.41	46.09	0.68	14.00
6-Hydroxy	V_m	32.7		25.6	
	K_m	48.6		43.1	
	CL_{int}	0.67	21.98	0.59	12.31
4′-*O*-Demethyl	V_m	151.5		315.7	
	K_m	155.0		88.8	
	CL_{int}	0.98	31.93	3.56	73.69
	Sum CL_{int}	3.06	100	4.82	100

zole (Fig. 1 and Table I), with the significant differences in k_e, $t_{1/2}$, and MRT values between the two enantiomers. This implied that an enantioselective process was involved in the absorption, distribution, metabolism, or excretion of pantoprazole. The parent drug was observed to be only in trace amount in rat urine (23), which indicated that there was no difference in the processes of excretion of pantoprazole enantiomers. So the enantioselectivity in processes of absorption, distribution, and metabolism was investigated in this study.

In this study, the *in vivo* (in Wistar rats, Beagle dog, and in rat liver microsomes) chiral inversion of pantoprazole enantiomers has been investigated. The results show that chiral inversion of pantoprazole enantiomers in Wistar rats and Beagle dog after p.o. or i.v. administration and in rat liver microsomes was not observed (data were not presented). However, Masubuchi *et al.* (18) have reported that significant chiral inversion occurred after i.v. and p.o. administration of *R*-pantoprazole to male Sprague–Dawley rats. We have reported that *R*-pantoprazole did not inverse to *S*-pantoprazole in humans after oral administration (24). Mano *et al.* (25) have reported that, after oral administration of rabeprazole enantiomers to Beagle dog, the chiral inversion did not occur. Stenhoff *et al.* (26) have found that *S*-omeprazole could not chiral-inverse to *R*-omeprazole in humans. Thus, the chiral inversion of PPIs may be related to administration route and animal species.

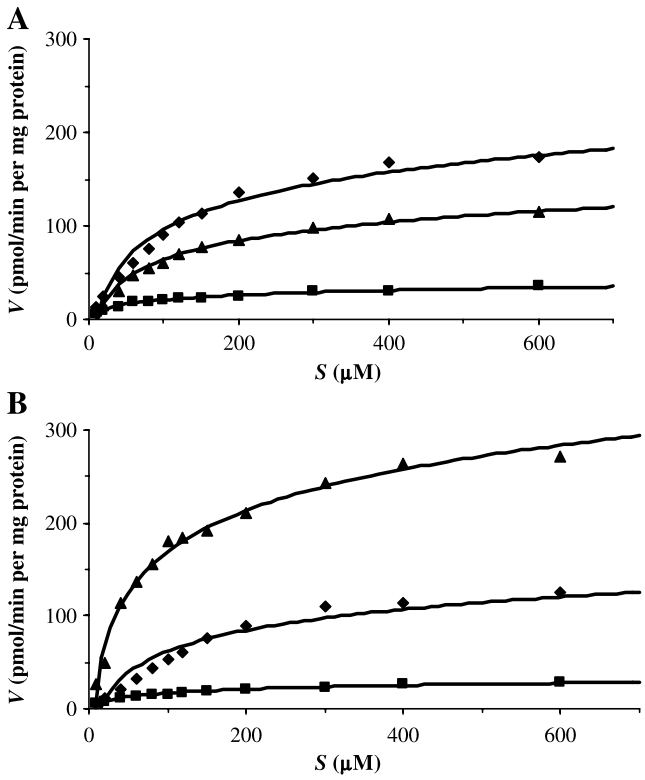

Fig. 4. Representative plots of the formation of sulfone (-♦-), 6-hydroxy (-■-), and 4′-*O*-demethyl (-▲-) from *S*-pantoprazole (A) and *R*-pantoprazole (B) in pooled rat liver microsomes (symbols are experimentally determined values, whereas solid lines are the computer-generated curves of best fit).

Absorption of both enantiomers from the small intestine was relatively rapid with similar t_{max} values (approximately 12 min). Whether or not pantoprazole enantiomers were absorbed enantioselectively has been examined. The *in situ* absorption study showed no evidence of enantioselective absorption of the two enantiomers from the intestine.

The binding extent of drugs to plasma protein is an important factor in tissue distribution because only unbound drugs can permeate biomembranes. *In vitro* and *in vivo* experiments have shown that pantoprazole has a high plasma protein binding (approximately 98%) (27). In this study, the extent of protein binding of *S*-pantoprazole was slightly greater than that of *R*-pantoprazole (Fig. 2). However, there was no significant difference in the unbound fraction between the two enantiomers of pantoprazole ($n = 5$, $p > 0.05$). Therefore, protein binding of pantoprazole enantiomers might not influence the enantioselective disposition of pantoprazole after oral administration.

There is a possibility of enantioselectivity in the liver metabolism of pantoprazole enantiomers as reported on other PPIs, i.e., omeprazole (13), lansoprazole (14–16), and H 285/31 (17). The optical isomers of pantoprazole show a clear difference in their metabolism by rat liver microsomes. The sum of the CL_{int} values for the three metabolites was considerably lower for *S*-pantoprazole than for *R*-pantoprazole. The slower metabolism of *S*-pantoprazole was indeed reflected in a 1.5-fold higher AUC *in vivo* for *S*-pantoprazole than for *R*-pantoprazole when given orally as racemic pantoprazole to Wistar rats. The CL_{int} of 4′-*O*-demethylpantoprazole sulfide formed from *R*-pantoprazole was significantly higher than that formed from *S*-pantoprazole, which was consistent with previous results obtained from *in vitro*

metabolism of other PPIs (17), whereas the CL_{int} of pantoprazole sulfone formed from *S*-pantoprazole were significantly higher than that formed from *R*-pantoprazole. This study suggested that there was enantioselectivity in the metabolism of pantoprazole enantiomers in rat liver microsomes.

In conclusion, it was shown that metabolism of pantoprazole in rat liver microsomes was enantioselective, which contributed to the different pharmacokinetics of pantoprazole enantiomers after oral administration of racemic pantoprazole to Wistar rats. *S*-Pantoprazole was favored to the formation of pantoprazole sulfone and 6-hydroxy-pantoprazole, whereas *R*-pantoprazole was favored to the formation of 4′-*O*-demethyl-pantoprazole sulfide.

ACKNOWLEDGMENT

This work was supported in part by Grant 2003-AA2Z347C of the "863" Program of China.

REFERENCES

1. P. Lindberg, P. Nordberg, T. Alminger, A. Brandstrom, and B. Wallmark. The mechanism of action of the gastric acid secretion inhibitor omeprazole. *J. Med. Chem.* **29**:1327–1329 (1986).
2. A. Fitton and L. Wiseman. Pantoprazole: a review of its pharmacological properties and therapeutic use in acid-related disorders. *Drugs* **51**:460–482 (1996).
3. P.W. Jungnickel. Pantoprazole: a new proton pump inhibitor. *Clin. Ther.* **22**:1268–1293 (2000).
4. W. A. Simon. Pantoprazole—Which cytochrome P450 isoenzymes are involved in its biotransformation. *Gut* **37**(Suppl. 2): A135(1995).
5. A. M. Cairns, R. H. Chiou, J. D. Rogers, and J. L. Demetriades. Enantioselective high-performance liquid chromatographic determination of omeprazole in human plasma. *J. Chromatogr.* **666**:323–328 (1995).
6. G. Tybring, Y. Bottiger, J. Widen, and L. Bertilsson. Enantioselective hydroxylation of omeprazole catalyzed by CYP2C19 in Swedish white subjects. *Clin. Pharmacol. Ther.* **62**:129–137 (1997).
7. M. Tanaka, T. Ohkubo, K. Otani, A. Suzuki, S. Kaneko, K. Sugawara, Y. Ryokawa, and T. Ishizaki. Stereoselective pharmacokinetics of pantoprazole, a proton pump inhibitor, in extensive and poor metabolizers of *S*-mephenytoin. *Clin. Pharmacol. Ther.* **69**:108–113 (2001).
8. M. Tanaka, H. Yamazaki, H. Hakusui, N. Nakamichi, and H. Sekino. Differential stereoselective pharmacokinetics of pantoprazole, a proton pump inhibitor in extensive and poor metabolizers of pantoprazole: a preliminary study. *Chirality* **9**:17–21 (1997).
9. H. Katsuki, H. Yagi, K. Arimori, C. Nakamura, M. Nakano, S. Katafuchi, Y. Fujioka, and S. Fujiyama. Determination of *R*(+)- and S(−)-lansoprazole using chiral stationary-phase liquid chromatography and their enantioselective pharmacokinetics in humans. *Pharm. Res.* **13**:611–615 (1996).
10. K. Kim, J. Shon, J. Park, Y. Yoon, M. Kim, D. Yun, M. Kim, I. Cha, M. Hyun, and J. Shin. Enantioselective disposition of lansoprazole in extensive and poor metabolizers of CYP2C19. *Clin. Pharmacol. Ther.* **72**:90–99 (2002).
11. S. Takakuwa, S. Chiku, H. Nakata, T. Yuzuriha, N. Mano, and N. Asakawa. Enantioselective high-performance liquid chromatographic assay for determination of the enantiomers of a new anti-ulcer agent, E3810, in Beagle dog plasma and rat plasma. *J. Chromatogr., B* **673**:113–122 (1995).
12. N. Mano, Y. Oda, S. Takakuwa, S. Chiku, H. Nakata, and N. Asakawa. Plasma direct injection high-performance liquid chromatographic method for simultaneous determining E3810 enantiomers and their metabolites by using flavoprotein-conjugated column. *J. Pharm. Sci.* **85**:903–907 (1996).
13. A. Abelo, T. B. Andersson, M. Antonsson, A. K. Naudot, I. Skanberg, and L. Weidolf. Stereoselective metabolism of omeprazole by human cytochrome P450 enzymes. *Drug Metab. Dispos.* **28**:966–972 (2000).
14. K. Arimori, K. Yasuda, H. Katsuki, and M. Nakano. Pharmacokinetic differences between lansoprazole enantiomers in rats. *J. Pharm. Pharmacol.* **50**:1241–1245 (1998).
15. K. Masa, A. Hamada, K. Arimori, J. Fujii, and M. Nakano. Pharmacokinetic differences between lansoprazole enantiomers and contribution of cytochrome P450 isoforms to enantioselective metabolism of lansoprazole in dogs. *Biol. Pharm. Bull.* **24**:274–277 (2001).
16. K. A. Kim, M. J. Kim, J. Y. Park, J. H. Shon, Y. R. Yoon, S. S. Lee, K. H. Liu, J. H. Chun, M. H. Hyun, and J. G. Shin. Stereoselective metabolism of lansoprazole by human liver cytochrome P450 enzymes. *Drug Metab. Dispos.* **31**:1227–1234 (2003).
17. A. Abelo, T. B. Andersson, U. Bredberg, I. Skanberg, and L. Weidolf. Stereoselective metabolism by human liver CYP enzymes of a substituted benzimidazole. *Drug Metab. Dispos.* **28**:58–64 (2000).
18. N. Masubuchi, H. Yamazaki, and M. Tanaka. Stereoselective chiral inversion of pantoprazole enantiomers after separate doses to rats. *Chirality* **10**:747–753 (1998).
19. H. Hirayama, X. Xu, and K. S. Pang. Viability of the vascularly perfused, recirculating rat intestine and intestine–liver preparations. *Am. J. Physiol.* **257**:G249–G258 (1989).
20. L. Ernster, P. Siekevitz, and G. E. Palada. Enzyme–structure relationships in the endoplasmic reticulum of rat liver. *J. Cell Biol.* **15**:541–562 (1962).
21. O. H. Lowry, N. J. Rosebrough, A. L. Farr, and R. J. Randall. Protein measurement with the folin phenol reagent. *J. Biol. Chem.* **193**:175–265 (1951).
22. K. Yanaoka, Y. Tanigawara, T. Nakagawa, and T. Iga. A pharmacokinetic analysis program (MULTI) for microcomputer. *J. Pharmacobio-Dyn.* **4**:879–885 (1981).
23. D. F. Zhong, Z. Y. Xie, and X. Y. Chen. Metabolism of pantoprazole involving conjugation with glutathione in rats. *J. Pharm. Pharmacol.* **57**:341–349 (2005).
24. Z. Y. Xie, B. H. Yang, Y. F. Zhang, and D. F. Zhong. Studies on chiral inversion of dextro-pantoprazole in human. *Acta Pharm. Sin.* **39**:370–373 (2004).
25. N. Mano, Y. Oda, S. Takakuwa, T. Yuzuriha, N. Mano, and N. Asakawa. Plasma direct injection high-performance liquid chromatographic method for simultaneously determining E3810 enantiomers and their metabolites by using flavoprotein-conjugated column. *J. Pharm. Sci.* **85**:903–907 (1996).
26. H. Stenhoff, A. Blomqvist, and P. O. Lagerstrom. Determination of the enantiomers of omeprazole in blood plasma by normal-phase liquid chromatography and detection by atmospheric pressure ionization tandem mass spectrometry. *J. Chromatogr., B* **734**:191–201 (1999).
27. R. Huber, B. Kohl, G. Sachs, J. Senn-Bilfinger, W. A. Simon, and E. Sturm. The continuing development of proton pump inhibitor, with particular reference to pantoprazole. *Aliment. Pharmacol. Ther.* **9**:363–378 (1995).